ALTERED HUB CONFIGURATIONS DURING PROPOFOL-INDUCED LOSS OF CONSCIOUSNESS

Huandong Li[1], Xiaoyuan Liu[2], Nanfeng Jie[1], Baoguo Wang[3], Tianzi Jiang [1]

[1]Brainnetome Center, Institute of Automation, Chinese Academy of Sciences, Beijing 100190, China. E-mail: hdli@nlpr.ia.ac.cn
[2]Capital University of Medical Sciences Affiliated Tiantan Hospital, Beijing 100050, China. E-mail: lxy13621278793@163.com.
[3]Department of Anesthesiology, Sanbo Brain Hospital, Capital Medical University, Beijing 100093, China. E-mail: wangbg605@sina.com.

Keywords: propofol, functional MRI, hub, graph theory, consciousness

Abstract

Graph-theoretical analysis of human brain functional networks based on functional magnetic resonance imaging (fMRI) have supported the existence of highly connected hub regions that may play a key role in brain function and cognition. Here, we investigated the hub distributions of 16 healthy volunteers during wakefulness and propofol-induced loss of consciousness (both light sedation and deep sedation). Functional connectivity between 160 cortical and subcortical regions was measured by correlation analysis and then thresholded to construct undirected graphs. We found that during wakefulness state highly connected hubs included bilateral angular, precuneus, posterior cingulate (PCC), superior frontal gyrus (SFG), ventrolateral frontal cortex (vFC), supplementary motor area (SMA) and pre-SMA, most of the which were in the default-mode network (DMN). However, during light sedation, we observed that hubs were mainly in posterior part of the brain (inferior parietal lobule, inferior temporal, occipital). And the major hubs during deep sedation were in the occipital lobe and cerebellum. Compared with wakefulness, the hub structures were significantly changed from heteromodal association cortex to unimodal association and primary cortices. Our findings support a reduction in integrated information and a topological reconfiguration during decreasing levels of consciousness.

1 Introduction

Propofol is the most widely used sedative-hypnotic agent in clinical procedures. It suppresses memory and consciousness with increasing dose, and induces to gradual changes in consciousness until consciousness is lost. However, the precise mechanisms by which propofol takes effect remain disputable. Recent research has suggested that disrupting cortical information integration is associated with anesthetic-induced unconsciousness [12, 20, 21, 25].

Studies of consciousness are increasingly focusing on large-scale networks rather than the single brain areas. Resting-state functional magnetic resonance imaging (rs-fMRI) is an efficient tool to detect the temporal coherence of fMRI signals between remote regions [3]. Recently, the combination of rs-fMRI and graph theoretic analysis, which can reveal the topological organization of human large-scale functional networks in the human brain, has been widely used in the studies of propofol-induced loss of consciousness [10, 15-17, 20, 21].

Hubs, which are central and highly connected regions, play a crucial role in the information communication of the brain's networks. A recent study suggests that global topological properties are homeostatically conserved while hub structures are reorganized in comatose patients [2]. Similar results were also found in healthy subjects after propofol-induced unconsciousness [15]. These results imply that the hub regions might be the key to unravelling the mystery of consciousness.

In this study, we applied graph theory based on rs-fMRI to investigate changes in hub structures and functional connectivity across awake, light sedation and deep sedation states of subjects. Our results suggest that major hubs were reconfigured as subjects move from wakefulness to deep sedation, which may be related to the changes in consciousness. Our findings indicate a reduction in information integration and a topological reconfiguration during decreasing levels of consciousness.

2 Materials and methods

2.1 Subject information

This study included sixteen healthy, right-handed participants (8 male; age range, 18-40 year; mean age ± SD, 25.3 ± 7.4 year; weight range, 48-75 kg; mean weight ± SD, 58 ± 8 kg), who were recruited through local advertisements and acquaintances. None of the subjects had a history of any psychiatric or neurological illness, or drug addiction. The Medical Research Ethics Committee of Tiantan Hospital approved all experimental procedures and protocols in this research. All subjects gave written informed consent after been fully explained about the purpose of this study.

2.2 Sedation protocol

Participants fasted for at least 6 hours from solids and 4 hours from liquids prior to the experiments. The anesthetic agent,

propofol, was administrated using a TCI pump (Base Primea Orechestra drug infusion workstation, Fresenius Kabi Pharmaceutical Co., Ltd., Model: MODULE DPS ORCHESTRA IS3) coupled with the assessment of OAA/S (observer's assessment of alertness/sedation) scores. Light sedation was induced to achieve plasma concentration of 1.0 μg/ml while the OAA/S was closed to 4, and deep sedation was induced to achieve 3.0 μg/ml while OAA/S score reached 2-3 points. Once the concentration was achieved at light or deep sedation state and kept stable for another 10 minutes, the level of consciousness was evaluated clinically with the OAA/S scores. Then a 5 minutes fMRI equilibration period was established. Throughout the experiment, Blood pressure (MAP), pulse oxymetry (SpO2), Electrocardiogram (ECG), and end-tidal carbon dioxide (etCO2) were continuously monitored.

2.3 MR data acquisition

All MR images were collected on a Siemens 3-T scanner (Magnetom Trio, Siemens, Erlangen, Germany). Rubber earplugs and foam pad were used to minimize scanner noise and potential head movements. A three-dimensional magnetization-prepared rapid gradient echo (MPRAGE) was first performed to obtain anatomical images for each volunteer. Functional images of the whole brain were acquired using an echo-planar imaging sequence (TR/TE = 2000/30 ms; FA = 90°; FOV = 256 mm × 256 mm; matrix size = 64 × 64; slice thickness/gap = 4.0/0.0 mm; voxel size = 4.0mm × 4.0mm × 4.0 mm; 32 transversal slices; 150 volumes). The fMRI scanning were repeated during each consciousness state (wakefulness, light sedation, deep sedation).

2.4 Data preprocessing

The fMRI images were preprocessed using Statistical Parametric Mapping (SPM8, http://www.fil.ion.ucl.ac.uk/spm) and Data Processing Assistant for Resting-State fMRI (DPARSF; [6]). Briefly, the first 5 volumes of each session were discarded to allow for magnetization equilibrium. The remaining fMRI images were then preprocessed as follows : slice-timing, realigning to the first volume to correct head motion; normalizing to the standard EPI template in MNI space and resampling to 3-mm^3 voxels; spatial smoothing using a 6-mm full-width at half-maximum Gaussian kernel; regressing nuisance variances (6 head motion parameters, linear drift, global mean, white matter and cerebrospinal fluid signals); and finally, temporal filtering (0.01-0.1 Hz) was performed[3]. Two participants were excluded due to excessive head movements (> 2 mm or > 2^o). Two subjects who did not finish the fMRI scanning at deep sedation were also excluded. To summarize, the final group size of participants was 12 who had three fMRI sessions.

2.5 Functional network construction

Functional networks consist of nodes and edges. In this study, nodes are 160 10-mm diameter functional regions of interest (ROIs) provided by a prior meta-analysis of fMRI activation study [8]. These 160 ROIs were modularized into six networks, including the cerebellar, cingulo-opercular, DMN, fronto-parietal, occipital, and sensorimotor networks [8]. This parcellation approach defines segregated ROIs which covered most of the cortex and involved the most of the intrinsic networks. Then network matrices were constructed for each subject by calculating functional connectivity between all possible pairs of the ROIs using Pearson's correlation coefficient. For the further statistical analysis of functional connectivity, the connectivity matrices were transformed into z-values using the Fisher's r-to-z transformation. To generate the Group-averaged brain networks, we first averaged the subject-specific networks. To remove weak correlations, we then performed one-sample t-test for each group and applied a threshold so that only the correlations whose p values were below a statistical threshold ($p<0.05$) were retained. Considering the negative correlations induced by the removal of global mean signal, we set the negative correlations to their absolute values. Finally, three weighted, undirected and positive group-averaged functional networks were generated.

2.6 Graph-theoretical analyses and hubness

"Hubs" are the most central or influential nodes and hold key positions in a network [5, 22, 23]. It should be noted that no consensus has been reached regarding the best way of detecting these hubs. Indeed, multiple influence measures (e.g., degree, betweenness, clustering coefficient, characteristic path length, and global efficiency) have to be considered to identify hub nodes [13, 14, 18, 22, 26]. Here, we identified nodes as hubs using a rule-of-thumb method for which their connectivity strength *s* and node global efficiency *e* were at least one standard deviation above the mean of all nodes in the network [11,14]. Specifically, the nodal strength Si was calculated as the sum of the weights of all the connections of node *i*. The nodal global efficiency *Ei* was computed as the inverse of the mean shortest path length between *i* and all other nodes[1]. The analysis of graph theoretical properties were carried out using the Graph Theoretical Network Analysis Toolbox (GRETNA; [27]). Figures in this article were produced by using The BrainNet Viewer [28].

3 Results

3.1 Physiological variables

Vital signs did not change significantly in the wakefulness state, light sedation and deep sedation states. The OAA/S scores gradually decreased with increasing dose of propofol (Table 1).

3.2 Functional hub structures at different level of consciousness

In this study, if a node has both high strength and global efficiency (> mean + SD), it is considered as a hub. During normal wakefulness, 23 hubs were identified (Figure 1 and

Parameter	Wakefulness	Light Sedation	Deep Sedation
MAP (mmHg)	88 ± 8	82 ± 8	75 ± 7
HR (bpm)	66 ±9	64 ± 7	68 ± 8
SpO2 (%)	100 ± 0	99 ± 1	98 ± 2
EtCO2 (%)	38.1 ± 2.4	38.9 ± 2.1	44.3± 2.7
OAA/S	5 ± 0	4 ± 0.2	2 ± 0.4

Table 1: Physiological variables and OAA/S scores
Results are expressed as mean ± standard deviation of individual values in each state.

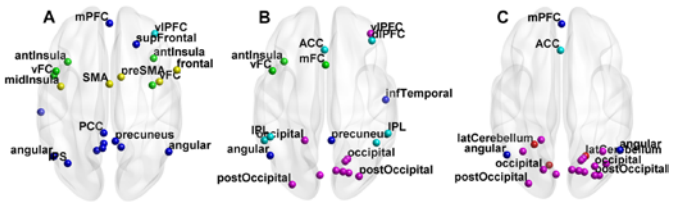

Figure1: Hub distributions are shown for the wakefulness (A), light sedation (B) and deep sedation (C) state (cerebellum, red; cingulo-opercular, green; DMN, blue; fronto-parietal, cyan; occipital, violet; and sensorimotor, yellow).

Label	ROI #	Network	MNI coordinates		
			X	Y	Z
ant insula	21	cingulo-opercular	38	21	-1
ant insula	22	cingulo-opercular	-36	18	2
mid insula	31	cingulo-opercular	37	-2	-3
vFC	48	cingulo-opercular	-46	10	14
vFC	49	cingulo-opercular	-48	6	1
angular	52	default	51	-59	34
angular	53	default	-48	-63	35
inf temporal	57	default	-59	-25	-15
IPS	59	default	-36	-69	40
mPFC	60	default	0	51	32
PCC	68	default	-5	-43	25
PCC	69	default	-5	-52	17
PCC	70	default	10	-55	17
PCC	71	default	-11	-58	17
precuneus	74	default	5	-50	33
precuneus	75	default	-6	-56	29
sup frontal	77	default	23	33	47
vlPFC	104	fronto-parietal	39	42	16
frontal	129	sensorimotor	58	11	14
mid insula	131	sensorimotor	-42	-3	11
pre-SMA	152	sensorimotor	10	5	51
SMA	153	sensorimotor	0	-1	52
vFC	160	sensorimotor	43	1	12

Table 2: Hub regions in wakefuleness

Label	ROI #	Network	MNI coordinates		
			X	Y	Z
ant insula	22	cingulo-opercular	-36	18	2
mFC	30	cingulo-opercular	0	15	45
vFC	48	cingulo-opercular	-46	10	14
angular	53	default	-48	-63	35
inf temporal	56	default	52	-15	-13
precuneus	74	default	5	-50	33
ACC	85	fronto-parietal	-1	28	40
dlPFC	91	fronto-parietal	40	36	29
IPL	95	fronto-parietal	54	-44	43
IPL	96	fronto-parietal	-48	-47	49
IPL	97	fronto-parietal	-53	-50	39
IPL	98	fronto-parietal	44	-52	47
vlPFC	104	fronto-parietal	39	42	16
occipital	106	occipital	-18	-50	1
occipital	110	occipital	19	-66	-1
occipital	111	occipital	17	-68	20
occipital	116	occipital	9	-76	14
occipital	117	occipital	15	-77	32
occipital	118	occipital	20	-78	-2
post occipital	119	occipital	-5	-80	9
post occipital	120	occipital	29	-81	14
post occipital	123	occipital	-29	-88	8

Table 3: Hub regions in light sedation.

Label	ROI #	Network	MNI coordinates		
			X	Y	Z
lat cerebellum	10	cerebellum	-24	-54	-21
lat cerebellum	12	cerebellum	21	-64	-22
med cerebellum	16	cerebellum	-11	-72	-14
angular	52	default	51	-59	34
angular	53	default	-48	-63	35
mPFC	60	default	0	51	32
ACC	85	fronto-parietal	-1	28	40
occipital	106	occipital	-18	-50	1
occipital	107	occipital	-34	-60	-5
occipital	108	occipital	36	-60	-8
occipital	110	occipital	19	-66	-1
occipital	111	occipital	17	-68	20
occipital	112	occipital	39	-71	13
occipital	113	occipital	29	-73	29
occipital	115	occipital	-16	-76	33
occipital	116	occipital	9	-76	14
occipital	117	occipital	15	-77	32
occipital	118	occipital	20	-78	-2
post occipital	119	occipital	-5	-80	9
post occipital	120	occipital	29	-81	14
post occipital	121	occipital	33	-81	-2
post occipital	123	occipital	-29	-88	8

Table 4: Hub regions in deep sedation.

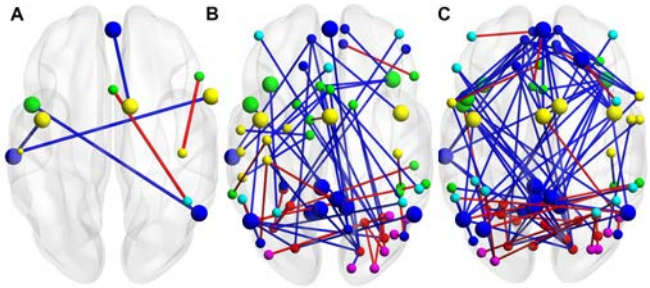

Figure 2: Changed interregional connectivity between wakefulness, light sedation and deep sedation with (A) wakefulness *vs*. light sedation, (B) light sedation *vs*. deep sedation comparison, and (C) wakefulness *vs*. deep sedation comparison. Cerebellum, red; cingulo-opercular, green; DMN, blue; fronto-parietal, cyan; occipital, violet; and sensorimotor, yellow. Blue lines represent decrease and red lines represent increase. ROIs with greater diameter are hubs in wakefulness.

Table2). Among these hubs, there were 12 hubs belonging to DMN, including PCC/precuneus, angular gyrus, medial prefrontal gyrus (mPFC) and superior frontal gyrus. The SMA, pre-SMA and insula were identified as hubs. This distribution of hubs were similar to those identified in previous fMRI studies in healthy people [4, 7, 24]. Compared with the awake state, when under light sedation, hubs in DMN were reduced, and more hubs were located at inferior parietal lobule (IPL) and occipital lobe (Figure1 and Table3). Moreover, during deep sedation, hubs were mainly brain areas in occipital lobe and cerebellum.

3.2 Disrupted hub-related functional connectivity during propofol-induced loss of consciousness

We applied a one-way repeated measures ANOVA to explore differences of functional connectivity between the three conditions. A post-hoc analysis was to be performed if significant differences were observed ($p < 0.001$). In total, 185 functional connections were found to be significantly different between awake, light sedation and deep sedation, mostly involving the hub regions. Nevertheless, when comparing wakefulness and light sedation, only several functional connections changed. However, when comparing wakefulness to deep sedation, we found that brain network had widespread deductions, especially the connection between parietal and frontal lobe. A more detailed representation of the results can be found in Figure 2.

4 Discussion and conclusions

In this study, we used rs-fMRI and graph-theoretical analysis to evaluate the hub distribution associated with the propofol-induced loss of consciousness. We found that hub structures were drastically affected by propofol. In normal awake state, hubs were in frontal and parietal areas in DMN which involved in a series of function processing and were closely correlated to maintenance of consciousness [9,19], as well as insula and sensorimotor areas. The hubs identified in normal awake state were consistent with previous studies [4,7,24]. As the dose was increased, hubs transferred from heteromodal association cortex in the anterior part of the brain to unimodal association and primary cortices in the posterior part. In addition, we observed systemic decreases in functional connectivity, particular inter-network connections. Most of the functional connectivity was hub-related. In summary, this study provides imaging evidence that propofol may suppress consciousness through reconfiguring hub structures and disrupting the functional integration.

References

[1] S. Achard, and E. Bullmore. “Efficiency and cost of economical brain functional networks”, *PLoS Comput Biol*, vol. 3, no. 2, pp. e17, 2007.

[2] S. Achard, C. Delon-Martin, P. E. Vertes, F. Renard, M. Schenck, F. Schneider, C. Heinrich, S. Kremer, and E. T. Bullmore. “Hubs of brain functional networks are radically reorganized in comatose patients”, *Proc Natl Acad Sci U S A*, vol. 109, no. 50, pp. 20608-20613, 2012.

[3] B. Biswal, F. Z. Yetkin, V. M. Haughton, and J. S. Hyde. “Functional connectivity in the motor cortex of resting human brain using echo-planar MRI”, *Magn Reson Med*, vol. 34, no. 4, pp. 537-541, 1995.

[4] R. L. Buckner, J. Sepulcre, T. Talukdar, F. M. Krienen, H. Liu, T. Hedden, J. R. Andrews-Hanna, R. A. Sperling, and K. A. Johnson. “Cortical hubs revealed by intrinsic functional connectivity: mapping, assessment of stability, and relation to Alzheimer's disease”, *J Neurosci*, vol. 29, no. 6, pp. 1860-1873, 2009.

[5] E. Bullmore, and O. Sporns. “Complex brain networks: graph theoretical analysis of structural and functional systems”, *Nat Rev Neurosci*, vol. 10, no. 3, pp. 186-198, 2009.

[6] Y. Chao-Gan, and Z. Yu-Feng. “DPARSF: A MATLAB Toolbox for "Pipeline" Data Analysis of Resting-State fMRI”, *Front Syst Neurosci*, vol. 4, pp. 13, 2010.

[7] Z. Dai, C. Yan, K. Li, Z. Wang, J. Wang, M. Cao, Q. Lin, N. Shu, M. Xia, Y. Bi, and Y. He. “Identifying and Mapping Connectivity Patterns of Brain Network Hubs in Alzheimer's Disease”, *Cereb Cortex*, 2014.

[8] N. U. Dosenbach, B. Nardos, A. L. Cohen, D. A. Fair, J. D. Power, J. A. Church, S. M. Nelson, G. S. Wig, A. C. Vogel, C. N. Lessov-Schlaggar, K. A. Barnes, J. W. Dubis, E. Feczko, R. S. Coalson, J. R. Pruett, Jr., D. M. Barch, S. E. Petersen, and B. L. Schlaggar. “Prediction of individual brain maturity using fMRI”, *Science*, vol. 329, no. 5997, pp. 1358-1361, 2010.

[9] D. Fernandez-Espejo, A. Soddu, D. Cruse, E. M. Palacios, C. Junque, A. Vanhaudenhuyse, E. Rivas, V. Newcombe, D. K. Menon, J. D. Pickard, S. Laureys, and A. M. Owen. “A role for the default mode network in the bases of disorders of

consciousness", *Ann Neurol*, vol. 72, no. 3, pp. 335-343, 2012.

[10] T. Gili, N. Saxena, A. Diukova, K. Murphy, J. E. Hall, and R. G. Wise. "The thalamus and brainstem act as key hubs in alterations of human brain network connectivity induced by mild propofol sedation", *J Neurosci*, vol. 33, no. 9, pp. 4024-4031, 2013.

[11] Y. He, J. Wang, L. Wang, Z. J. Chen, C. Yan, H. Yang, H. Tang, C. Zhu, Q. Gong, Y. Zang, and A. C. Evans. "Uncovering intrinsic modular organization of spontaneous brain activity in humans", *PLoS One*, vol. 4, no. 4, pp. e5226, 2009.

[12] A. Hudetz. "Cortical Disintegration Mechanism of Anesthetic-Induced Unconsciousness", *Suppressing the Mind*, Contemporary Clinical Neuroscience A. Hudetz and R. Pearce, eds., pp. 99-125: Humana Press, 2010.

[13] K. Hwang, M. N. Hallquist, and B. Luna. "The development of hub architecture in the human functional brain network", *Cereb Cortex*, vol. 23, no. 10, pp. 2380-2393, 2013.

[14] T. Itahashi, T. Yamada, H. Watanabe, M. Nakamura, D. Jimbo, S. Shioda, K. Toriizuka, N. Kato, and R. Hashimoto. "Altered network topologies and hub organization in adults with autism: a resting-state fMRI study", *PLoS One*, vol. 9, no. 4, pp. e94115, 2014.

[15] H. Lee, G. A. Mashour, G. J. Noh, S. Kim, and U. Lee. "Reconfiguration of network hub structure after propofol-induced unconsciousness", *Anesthesiology*, vol. 119, no. 6, pp. 1347-1359, 2013.

[16] U. Lee, M. Muller, G. J. Noh, B. Choi, and G. A. Mashour. "Dissociable network properties of anesthetic state transitions", *Anesthesiology*, vol. 114, no. 4, pp. 872-881, 2011.

[17] U. Lee, G. Oh, S. Kim, G. Noh, B. Choi, and G. A. Mashour. "Brain networks maintain a scale-free organization across consciousness, anesthesia, and recovery: evidence for adaptive reconfiguration", *Anesthesiology*, vol. 113, no. 5, pp. 1081-1091, 2010.

[18] J. Qin, M. Wei, H. Liu, J. Chen, R. Yan, L. Hua, K. Zhao, Z. Yao, and Q. Lu. "Abnormal hubs of white matter networks in the frontal-parieto circuit contribute to depression discrimination via pattern classification", *Magn Reson Imaging*, vol. 32, no. 10, pp. 1314-1320, 2014.

[19] P. G. Samann, R. Wehrle, D. Hoehn, V. I. Spoormaker, H. Peters, C. Tully, F. Holsboer, and M. Czisch. "Development of the brain's default mode network from wakefulness to slow wave sleep", *Cereb Cortex*, vol. 21, no. 9, pp. 2082-2093, 2011.

[20] M. S. Schroter, V. I. Spoormaker, A. Schorer, A. Wohlschlager, M. Czisch, E. F. Kochs, C. Zimmer, B. Hemmer, G. Schneider, D. Jordan, and R. Ilg. "Spatiotemporal reconfiguration of large-scale brain functional networks during propofol-induced loss of consciousness", *J Neurosci*, vol. 32, no. 37, pp. 12832-12840, 2012.

[21] J. Schrouff, V. Perlbarg, M. Boly, G. Marrelec, P. Boveroux, A. Vanhaudenhuyse, M. A. Bruno, S. Laureys, C. Phillips, M. Pelegrini-Issac, P. Maquet, and H. Benali. "Brain functional integration decreases during propofol-induced loss of consciousness", *Neuroimage*, vol. 57, no. 1, pp. 198-205, 2011.

[22] O. Sporns. "Structure and function of complex brain networks", *Dialogues Clin Neurosci*, vol. 15, no. 3, pp. 247-262, 2013.

[23] O. Sporns, C. J. Honey, and R. Kotter. "Identification and classification of hubs in brain networks", *PLoS One*, vol. 2, no. 10, pp. e1049, 2007.

[24] D. Tomasi, and N. D. Volkow. "Functional connectivity hubs in the human brain", *Neuroimage*, vol. 57, no. 3, pp. 908-917, 2011.

[25] G. Tononi. "Consciousness as Integrated Information: a Provisional Manifesto", *The Biological Bulletin*, vol. 215, no. 3, pp. 216-242, 2008.

[26] M. P. van den Heuvel, R. C. Mandl, C. J. Stam, R. S. Kahn, and H. E. Hulshoff Pol. "Aberrant frontal and temporal complex network structure in schizophrenia: a graph theoretical analysis", *J Neurosci*, vol. 30, no. 47, pp. 15915-15926, 2010.

[27] J. Wang, X. Wang, M. Xia, X. Liao, A. Evans, and Y. He. "GRETNA: a graph theoretical network analysis toolbox for imaging connectomics", *Front Hum Neurosci*, vol. 9, pp. 386, 2015.

[28] M. Xia, J. Wang, and Y. He. "BrainNet Viewer: a network visualization tool for human brain connectomics", *PLoS One*, vol. 8, no. 7, pp. e68910, 2013.